EFFECTS OF THE INTERACTION BETWEEN LOAD AND SOURCE INDUCTANCES OF MATRIX CONVERTERS AT RESONANCE FREQUENCY

Jordan G. Trapp, Eng.*, Felix A. Farret, Ph.D.**
*Post-Graduation Program in Electrical Engineering - PPGEE
Federal University of Santa Maria – UFSM, CEP 97110-900, Santa Maria – RS Brazil
e-mail: jordantrapp@yahoo.com.br
**Department of Electronics and Computation – DELC, Technological Center
Federal University of Santa Maria – UFSM, CEP 97110-900, Santa Maria – RS Brazil
e-mail: faf@ct.ufsm.br

Abstract **- This paper analyzes single-phase matrix converters to obtain the general resonant conditions of the interaction between load and source inductances. Also, it presents some practical ways to determine the effect of load and source inductance variations when the source inductance is comparable to the load inductance. The converter can be either directly fed from the secondary of a transformer or connected to the electric network. In this paper, it is presented some equivalent circuits for half period switching, the corresponding resonance equation of the matrix converter and some of the effects caused by variation of the involved inductances. In order to validate all equations, some practical and theoretical results with the load voltage at resonance are used to compare their waveforms.**

Keywords **- Equivalent circuit, matrix converter, load versus source resonance interaction.**

I. INTRODUCTION

For applications where converters must have a sinusoidal output , unitary power factor and low harmonic content, as in induction heating, the use of matrix converters become a good option, as discussed in [1]. Moreover, the converter can be directly fed from the electric network or from a transformer secondary, without any rectifying circuit. This paper shows the effects of the load and source inductance variations at the resonance frequency of matrix converters, as well as the variation effects of these inductances on converter operation.

Amongst these effects, it is noticed that the commutation mode of the converter may suffer alterations, from hard switching to soft switching. This fact depends directly on the resonance condition, that is, it depends on the interaction between load and source inductances.

Without resonance, the converter operates with hard switching, and at resonance, the turning off switching is operated at ZVS. To obtain the resonance condition, it is analyzed the equivalent circuit for half period switching, as in [6] and [7]. It is necessary to obtain a third order equivalent circuit of the matrix converter. From this circuit, it is obtained the second order equivalent circuit, as in [4], by impedance transformation as used in [2].

Figure 1 represents the converter implemented for the practical and theoretical simulations. Inductance L, resistance

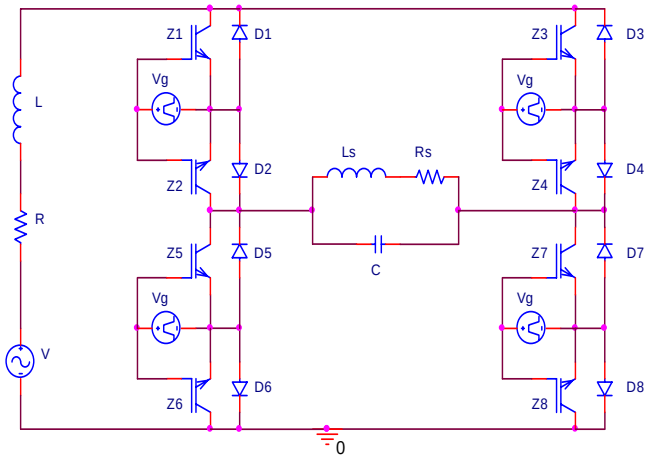

Fig. 1. Single-phase matrix converter with an RLC load

R and source V, are the source parameters.

Thus, L_s in series with R_s, both in parallel with capacitor C connected to L of the source, form the converter resonant circuit shown in figure 1. The second order circuit assures a simplified analysis for the converter, as well as in [5], to get the resonance equation.

II. RESULTS FROM THE MATHEMATICAL MODEL OF THE CONVERTER, SIMULATIONS AND PRACTICAL RESULTS

A. The 2nd and 3rd order equivalent circuits

The 3rd order equivalent circuit is obtained for the half period switching and at a frequency source a lot lower than the converter frequency. As the converter is bidirectional in current and voltage, the equivalent circuit behaves as being fed from a constant voltage source. The 3rd order equivalent circuit is shown in figure 2. Equations (1) to (5), as established in [2], are used to transform the intermediary series impedance in parallel impedance. The intermediary transformation follows as:

$$R_p = \frac{X_s^2 + R_s^2}{R_s} \quad (1)$$

and

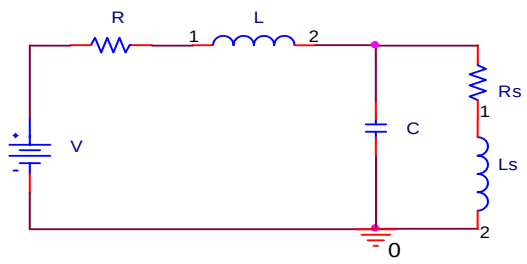

Fig. 2. Third order matrix converter equivalent circuit for the half period switching

$$X_p = \frac{X_s^2 + R_s^2}{X_s} \tag{2}$$

where:

R_s - load resistance
L_s - load inductance
X_s - load reactance
R_p - equivalent parallel resistance
L_p - equivalent parallel inductance
X_p - parallel reactance

With X_c and X_p, the equivalent reactance X_{Ceq} becomes:

$$X_{Ceq} = X_c - X_p \tag{3}$$

where:

X_C - capacitive reactance
X_{Ceq} - equivalent capacitive reactance

From equations (1) and (2), X_{Ceq} is defined as:

$$X_{Ceq} = X_c - \frac{X_s^2 + R_s^2}{X_s} \tag{4}$$

Therefore:

$$C_{eq} = C - \left(\frac{L_s}{(\omega L_s)^2 + R_s^2} \right) \tag{5}$$

where:

ω is the resonant angular frequency

Circuit shown in figure 3 is the equivalent circuit of the 2nd order matrix converter using equivalent capacitance *C*. It will be used to find the frequency resonance equation involving the inductor L, R_s, L_s and capacitor C.

Equations (6) to (18) are used to obtain the resonance equation of the circuit in figure 3.

$$V_o(s) = I_R(s) R_p \tag{6}$$

and

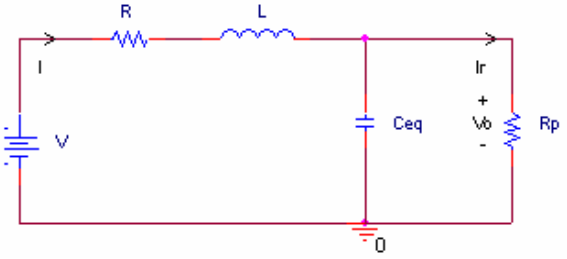

Fig. 3. Equivalent circuit of the 2nd order matrix converter using the equivalent capacitance C

$$V_o(s) = [I(s) - I_R(s)] \frac{1}{sC_{eq}} \tag{7}$$

thus

$$I(s) = I_R(s)\left(sC_{eq}R_p + 1\right) \tag{8}$$

therefore

$$V(s) = I(s)\left(sL + R\right) + \frac{1}{sC_{eq}}[I(s) - I_R(s)] \tag{9}$$

then

$$\frac{V_o(s)}{V(s)} = \frac{\frac{1}{LC_{eq}}}{s^2 + \left(\frac{1}{C_{eq}R_p} + \frac{R}{L}\right)s + \frac{R + R_p}{LC_{eq}R_p}} \tag{10}$$

Equation (10) is the transfer function of the output voltage related to the input voltage. Equation (11) is the characteristic equation of the final equivalent circuit given in figure 3.

$$s^2 + \left(\frac{1}{C_{eq}R_p} + \frac{R}{L}\right)s + \frac{R + R_p}{LC_{eq}R_p} = 0 \tag{11}$$

Considering that the classical solution of equation (11) is:

$$(s + \alpha)^2 + \beta^2 = 0 \tag{12}$$

and developing (12), yields:

$$s^2 + 2\alpha s + \alpha^2 + \beta^2 = 0 \tag{13}$$

Through a term by term analogy from equations (11) and (13), comes:

$$\alpha = \frac{1}{2C_{eq}R_p} + \frac{R}{2L} \tag{14}$$

and

$$\alpha^2 + \beta^2 = \frac{R + R_p}{LC_{eq}R_p} \tag{15}$$

defining

$$\beta^2 = \omega_o{}^2 - \alpha^2 \tag{16}$$

and, finally:

$$\beta^2 = \frac{R + R_p}{LC_{eq}R_p} - \left(\frac{1}{2C_{eq}R_p} + \frac{R}{2L}\right)^2 \tag{17}$$

thus

$$\omega_o = \sqrt{\frac{1 + R/R_p}{LC_{eq}}} \tag{18}$$

where ω_o is the natural oscillation frequency of the converter.

B. Simulations with the Matrix Converter

Simulations of the resonant circuits were carried out by the Orcad program, Version 9.2. The operating frequency, the source and load inductances and load resistances were defined as follows.

The necessary capacitance has to be determined so that the converter operates at resonance. The values used for R, R_s, L e L_s are: $R = 0.5\Omega$; $R_s = 0.1\Omega$; $L = 500uH$ and $L_s = 197uH$. The load frequency f_o is at 17.8kHz and the power source is at 60 Hz. To calculate C_{eq} it is necessary to previously calculate R_p at the resonance frequency. From equation (2) comes:

$$R_p = \frac{(2\pi \cdot 17800 \cdot 0.000197)^2 + 0.1^2}{0.1^2} = 48.5k\Omega$$

Thus, using equation (18) and isolating C_{eq}, comes:

$$C_{eq} = \frac{R + R_p}{LR_p\omega_o{}^2}, \text{ where } \omega_o = 2\pi f_o$$

thus

$$C_{eq} = \frac{0.5 + 48540}{0.0005 \cdot 48540 \cdot (2\pi 17800)^2} \cong 159.9nF$$

The resonant capacitor can be calculated through equation (5) as:

$$C = C_{eq} + \left(\frac{L_s}{(\omega_o L_s)^2 + R_s{}^2}\right) \cong 560nF$$

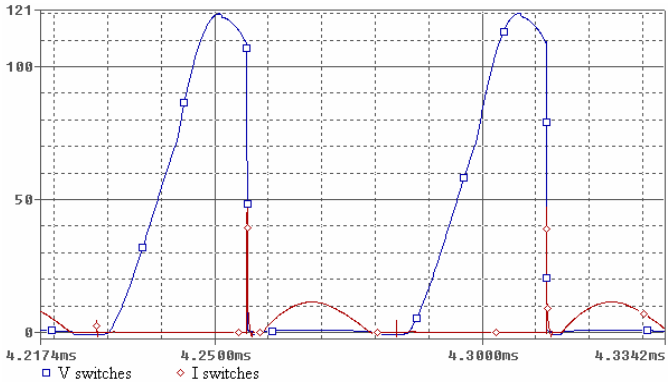

Fig. 4. Theoretical voltage across and current through switches with matrix converter at resonance

Digital simulations with the converter shown in figure 1 were carried out at a 17.8 kHz switching frequency at the load, duty cycle = 0.498 and values of inductors, resistances and capacitor are kept as already defined above. The voltage wave forms across and current through the switches are presented in figure 4, at the resonance, where the current was multiplied by 10 for the sake of clarity. Figure 5 shows an enlargement of voltage across switches for better visualization. In this situation, the switch turning-offs occur at zero voltage.

In Figure 4 it is also represented the current peaks with the corresponding voltage and current. These peaks occur during commutation of any converter switches. That is, as the simulator uses realistic models to represent the semiconductors, there are different recovering times associated to these components, as well as of the intrinsic parasite capacitances depending on the voltage they are submitted at. Exception is made for the diodes, whose junction capacitance has a practically constant value. So, the capacitor C is slightly discharged in a very short time, of the order of ns.

The capacitor discharge voltage is negligible when the load voltage wave levels are considered. With respect to capacitor current, where the current peaks through the switches and diodes, the converter loses the ZCS commutation condition. In Figure 10 is represented the equivalent circuit of the driving switches Z1, Z2, Z7 and Z8.

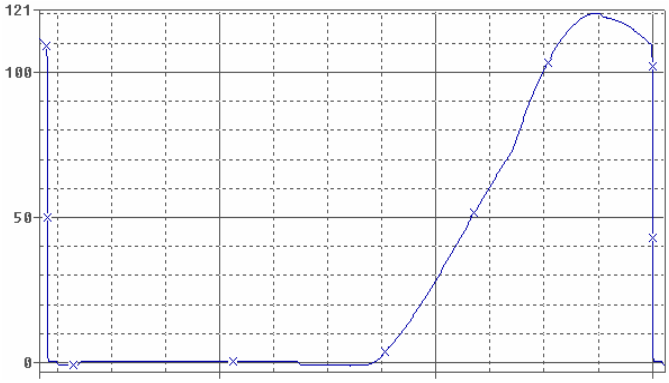

Fig. 5. Enlargement of the voltage across switches out of resonance

Figure 6 shows the load voltage and current at the resonance. The current was multiplied by 4 for better visualization.

At the commutation instant, C acts as a voltage source, and, as L represents high impedance, the current peaks caused by the capacitor discharge arise only through the converter parasite capacitances.

It is observable in figure 7 that the intrinsic capacitances across IGBTs are in series with the capacitance of the diode junction C_j. This equivalent capacitance diode/IGBT was taken as 308.7 pF. The current through the converter switches, in figure 4, show that every switch turning-on is not soft, therefore it has a voltage across the IGBT during current peaks caused by the discharges of *C*.

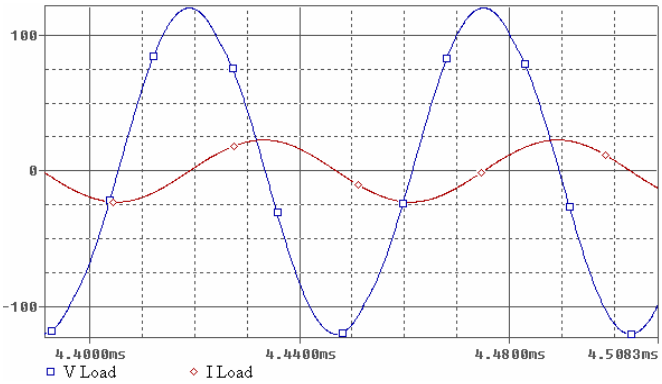

Fig. 6. Load voltage and current at the resonance

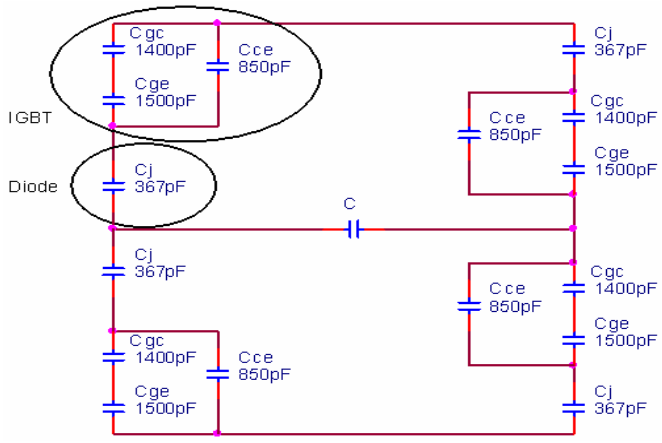

Fig. 7. Equivalent circuit of the converter during commutations

As an effect of the L_s inductance variation, the converter looses the resonant condition caused by an external factor, represented here to include the warming up effects of the metallic parts inside L_s inductor. In practice, occurs a variation of L_s from 197µH to 260µH for this situation. The load voltage remains essentially sinusoidal, but the electronic switches lose the ZVS condition at the turn off instant.

Figure 8 shows voltage across and current through the switches, where the current magnitude was multiplied by 5 for better visualization. Figure 9 represents an enlargement of the voltage across switches for better detailing.

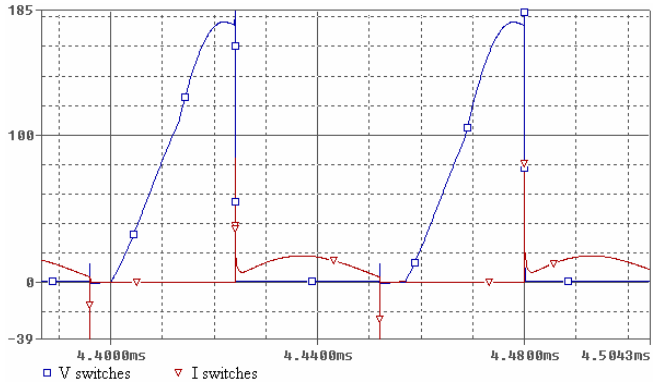

Fig. 8. Voltage across and current through switches out of resonance

It is noticeable the voltage surges during the switching offs (red encirclement). Figure 10 shows voltage across and current through the load, out of resonance. In figure 10 the current was multiplied by 4 for the better visualization.

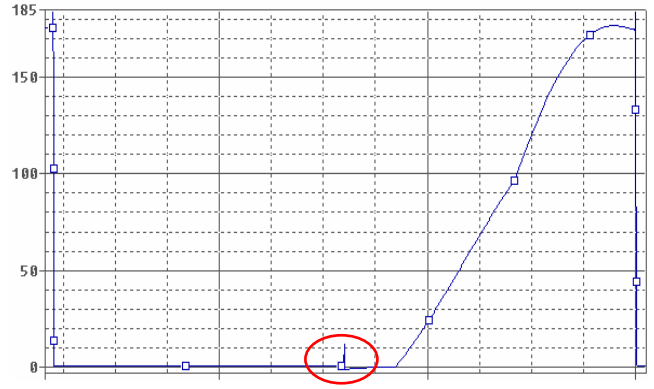

Fig. 9. Enlargement of the voltage across switches out of resonance

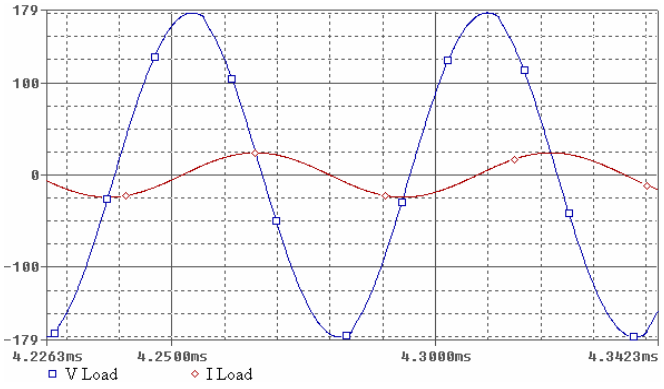

Fig. 10. Voltage across and current through load out of resonance

The current peaks also suffer alteration, increasing out of the resonance condition. That may be observed by comparing figures 4 and 8.

C. Practical Results

The slight difference between simulation results and practical results occurred only in relation to voltage and current levels but not in the wave forms.

This occurs because of the modeling limitations used in the practical converter, as for example, those due the parasite inductances, capacitances and resistances associated to the semiconductor devices, printed board layout, power source and load connections, circuits control and others, whose have to me considered in a more accurate power converter equivalent circuit. Figure 11 represents voltage across and current through the switches at resonance condition.

It is shown in figure 12 the switches voltage enlargement of the figure 11 and the figure 13 shows the load voltage and current at the resonance. The utilized current sensor was used in the 100mV/A scale and applied in the oscilloscope channel 2. The figures 14, 15 and 16 was obtained with the converter operates out of resonance, with L_s altered.

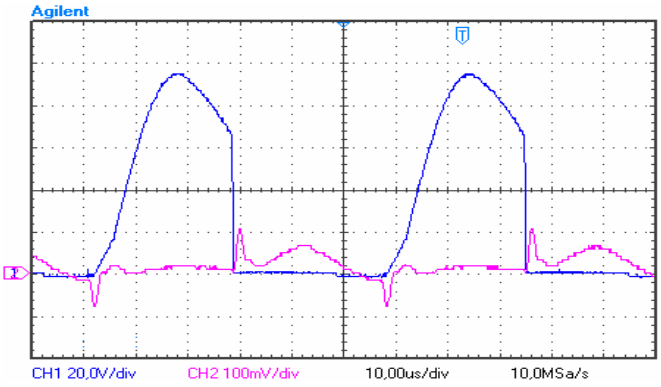

Fig. 11. Practical voltage across and current through the switches at resonance

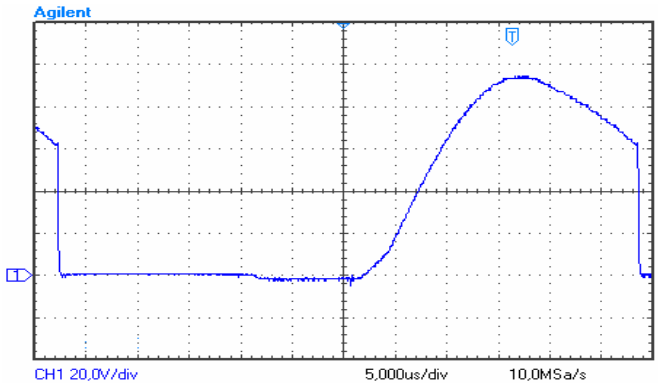

Fig. 12. Voltage across the switches at resonance

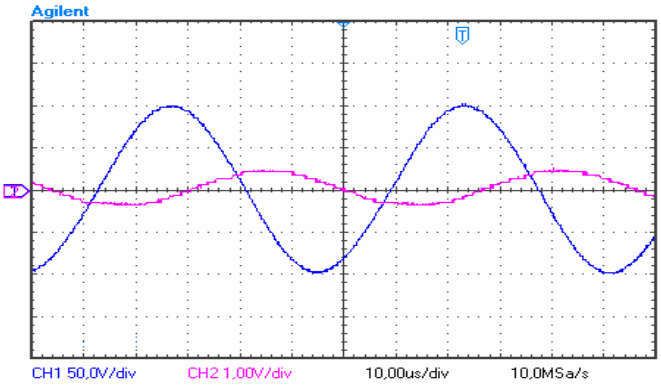

Fig. 13. Voltage across and current through the load at resonance

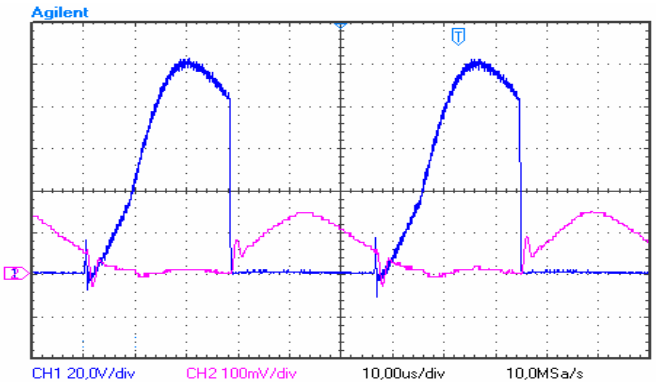

Fig. 14. Voltage across and current through the switches out of resonance

Practical voltage across and current through the switches are seen in figure 14. Figure 15 shows an enlargement of the voltage level across the converter switches. A voltage peak across every switch occurs at the switch turning-offs, and increasing de switching converter losses. It is noticeable the voltage surges during the switching offs (red encirclement). It is also observed in figure 14 that the current through the switches increases out of resonance. Figure 16 shows that the voltage across and current through the load, where the current is lower compared to those values at the resonance condition. The used current sensor works with 100kHz maximum frequency. Then, the current peaks can have a bigger value in relation to the measured values.

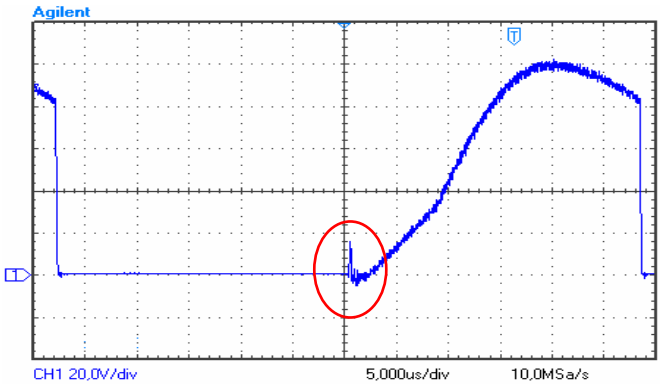

Fig. 15. Voltage across the switches out of resonance

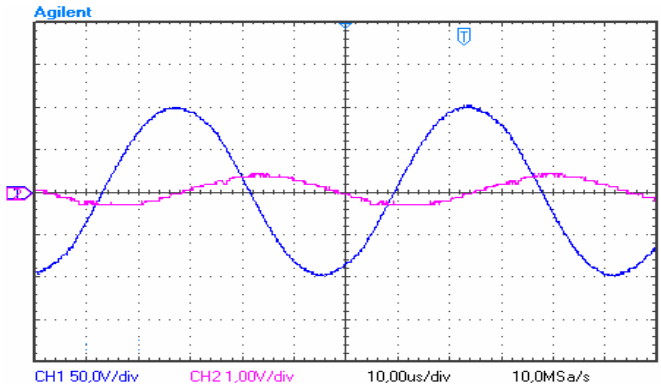

Fig. 16. Practical voltage across and current through the load out of resonance

III. CONCLUSIONS

The simulation results validate the modeling effects of the interaction between load and source inductances at the resonance frequency in matrix converters. Variations of load and source inductances have direct influence on the converter resonance frequency, where ω_o becomes dependent on L and L_s, this one is intrinsic to C_{eq}. Although only L_s varied, that is enough to alter the resonance frequency. During commutations, the converter as a bidirectional device in current and voltage, offers discharging current paths for the parasite capacitances of the component associated to the load capacitance *C*. So, current peaks are generated through the electronic switches causing an operation out of the ZCS condition. At resonance, the converter presents ZVS turning off condition but, out of resonance, this condition is lost. Differences do exist between simulated and practical results because the simulated converter was not represented in all its details due to the practical complexity and difficulties to get all the involved parameters for the implemented converter. However, the practical and theoretical wave forms resemble satisfactorily and show that the effect of the load inductance variation on the converter operation must be taken into consideration.

Acknowledgements

The authors are very thankful to CNPq-Brazil for their financial support and to the Post-Graduation Program in Electrical Engineering (PPGEE), Center of Research and Development in Electrical Engineering (NUPEDEE), and Center of Studies in Energy and Environment (CEEMA) of the Federal University of Santa Maria (UFSM).

References

[1] N. Nguyen-Quang, D.A. Stone, C.M. Bingham, and M.P. Foster, Single Phase Matrix Converter for Radio Frequency Induction Heating, International Symposium on Power Electronics, Electrical Drives, Automation and Motion, SPEEDAM 2006.

[2] Simões, M.G. and Farret, F.A., Renewable Energy Systems - Design and Analysis with Induction Generators - CRC Press, Boca Raton, Florida, EUA, 2004.

[3] Power Electronics: Converters, Applications, and Design, Mohan, N., Undeland, T.M. and Robbins, W.P., John Wiley & Sons, Inc., Minnesota, Minneapolis, EUA, 1989.

[4] Shenkman, A.L., Axelrod, B. and Chudnovsky, V., A New Simplified Model of the Dynamics of the Current-Fed Parallel Resonant Inverter, IEEE Transactions On Industrial Electronics, Vol. 47, no. 2, Apr/2000.

[5] Ivensky, G., Bronstein, S. and Ben-Yaakov, S., Approximate Analysis of the Resonant LCL DC-DC Converter, 23rd IEEE Israel Convention, pp. 4-48, Tel-Aviv, 2004.

[6] Patrick Hu, A., Covic, G.A. and Boys, J.T., Direct ZVS Start-Up of a Current-Fed Resonant Inverter, IEEE Transactions on Power Electronics, Vol. 21, no. 3, May/2006.

[7] Zhu Jianhua, Luo Fang Lin, Analysis of a Bipolar Current Source Resonant Power Inverter, IEEE, 2003.

[8] International Rectifier datasheet on IGBTs and Diodes, 2007.

Jordan Gustavo Trapp, received his Electrical Engineer degree (2004) from the Federal University of Santa Maria (UFSM). Currently is student in the Post-Graduation Program in Electrical Engineering (PPGEE) of UFSM. Mr Jordan develops research in Center of Studies in Energy and Environment (CEEMA) of the Technological Center, UFSM. His interest areas are: integration of alternative sources of energy, power electronics, control and automation of electronic systems.

Felix Alberto Farret, received his B.E. and M.Sc. in Electrical Engineering from the Federal University of Santa Maria in 1972 and 1986, respectively; specialist in instrumentation and automation by the Osaka Prefectural Industrial Research Institute, Japan; M.Sc. by the University of Manchester, UK in 1981 and Ph.D. from the University of London, UK, in 1984 all in Electrical Engineering. He was operation and maintenance engineer for the State Company of Electrical Energy (CEEE) in the RGS state 1973-1974, Brazil. He is working in an interdisciplinary educational background related to power systems, power electronics, nonlinear controls and integration of renewable energies. He teaches at the Department of Electronics and Computation of the Federal University of Santa Maria, Brazil, committed to under-graduated and graduated activities and in research developments, since 1974. He was a visiting professor at Colorado School of Mines, Engineering Division, USA, 2002-2003. He published his first book in Portuguese Language titled Use of Small Sources of Electrical Energy (UFSM University Press, 1999), co-authored the book Renewable Energy Systems: Design and Analysis with Induction Generators (CRC Press, 2004) and authored the book Integration of Alternative Sources of Energy (John Wiley & Sons, 2006). Alternative sources of energy and engineering systems for distribution and industrial applications are focus of his present interests.